ATP-Lipids—Protein Anchor and Energy Source in Two Dimensions[⊥]

Lutz Schmitt[†] and Robert Tampé*[,†,‡]

Contribution from the Lehrstuhl für Biophysik E22, Physik Department, Technische Universität München, D-85748 Garching, Germany, and Max-Planck-Institut für Biochemie, Am Klopferspitz 18a, D-82158 Martinsried, Germany

Received November 27, 1995[⊗]

Abstract: The ubiquitous function of ATP as energy equivalent in nature has resulted in a common folding pattern of ATP-binding proteins. Their binding pocket tolerates modifications of the adenine ring to some extend, whereas those of the triphosphate group strongly affect the binding affinity. In consequence, immobilized C8- and N^6-modified ATP analogues are frequently used for affinity purification of ATPases or kinases. To combine this unique recognition principle with the fascinating properties of self-assembly, we have synthesized a novel class of hydrolyzable and nonhydrolyzable ATP-lipids where the nucleotides are covalently attached via C8- or N^6-position of the adenine ring to a synthetic lipid. These ATP-lipids were characterized by various enzyme assays in micellar solution, resulting in ATPase and competition activities that are comparable to their free counterparts. The specific docking of actin as a model of an ATP-binding protein to ATP-lipid monolayers was followed by film balance technique and epifluorescence microscopy. Based on this specific interaction, actin-supported membranes were generated to study shape transitions of vesicular systems. Due to the coupling of actin to ATP-lipid bilayers drastic changes in the viscoelastic properties and shape transitions were observed by phase contrast microscopy. These results underline the properties of these novel ATP-lipids as protein anchor or energy source in two dimensions. They can be applied either to form phantom cells, actin-supported membranes or to orient and crystallize ATP-binding proteins at lipid interfaces.

Introduction

Biofunctionalization of interfaces can be achieved either in an unspecific, the so-called physisorption, or in a specific way, the so-called chemisorption.[1,2] The unspecific immobilization, which is based mainly on electrostatic and hydrophobic interaction often affects the activity and function of the adsorbed proteins. In contrast, the denaturation can be bypassed by a specific immobilization and a defined orientation of the biomolecule at the interface. One prominent type of interfaces are lipids, because of their fundamental properties such as self-assembly, lateral organization, and variability. Moreover, nearly every surface can be coated and functionalized by lipid films using various transfer techniques. Examples for functional moieties of modified lipids are dinitrophenol,[3] novobiocin,[4] progesterone,[5] hydroxamates,[6] cofactors like biotin,[7] NAD^+,[8] or γ-phosphate linked desoxy-ATP,[9] peptides,[10] sugars,[11,12] proteins such as antibody fragments,[13,14] and chelators which are capable to bind histidine-tagged proteins.[15,16] Some of these functionalized lipids have been used successfully for two-dimensional crystallization of proteins at lipid monolayers, such as dinitrophenol for an IgG antibody,[17] γ-phosphate linked desoxy-ATP for ribonucleotide reductase,[9] biotin for streptavidin,[18] and novobiocin for DNA gyrase B subunit.[4]

Biotin-lipids are frequently used for the immobilization and the self-organization of proteins at interfaces. To expand the system to other proteins of interest, a streptavidin interface[19] and a chemical biotinylation of the biomolecule[20] are required which often lacks side-specificity and stoichiometry. As a result, the orientation of the bound molecule cannot be controlled. A more recent approach combines genetic engineering with self-assembly using a novel class of chelator lipids.[15,16] This concept opens up the possibility for the specific and reversible immobilization and orientation of the vast variety of histidine-tagged fusion proteins at chelator lipid interfaces.[21−25]

* Corresponding author: Robert Tampé, Max-Planck-Institut für Biochemie, Am Klopferspitz 18a, D-82158 Martinsried, Germany. Phone: 0049-89-8578-2646. Fax: 0049-89-8578-2641. E-mail: tampe@vms.biochem.mpg.de.

† Technische Universität München.

‡ Max-Planck-Institut für Biochemie.

⊥ Keywords: actin, ATPases, ATP-binding, biofunctionalization, kinases, membranes, molecular recognition, self-assembly, self-organization.

⊗ Abstract published in *Advance ACS Abstracts,* May 15, 1996.

(1) Ulman, A. *An introduction to ultrathin organic films*; Academic Press: San Diego, CA, 1991.

(2) Tampé, R.; Dietrich, C.; Gritsch, S.; Elender, G.; Schmitt, L. *Nanofabrication and Biosystems: Integrating material science, engineering, and biosystems*; Cambridge University Press: Cambridge, 1996; in press.

(3) Weis, R. M.; Balakrishnan, K.; Smith, B. A.; McConnell, H. M. *J. Biol. Chem.* **1982**, *257*, 6440−6445.

(4) Lebeau, L.; Regnier, E.; Schultz, P.; Wang, J. C.; Mioskowski, C.; Oudet, P. *FEBS Lett.* **1990**, *267*, 38−42.

(5) Lebeau, L.; Oudet, P.; Mioskowski, C. *Helv. Chim. Acta* **1991**, *74*, 1697−1706.

(6) Altenburger, J.-M.; Lebeau, L.; Mioskowski, C. *Helv. Chim. Acta* **1992**, *75*, 2538−2544.

(7) Bayer, E. A.; Rivnay, B.; Skutelesky, E. *BBA* **1979**, *550*, 464−473.

(8) Salord, J.; Tarnus, C.; Muller, C. D.; Schuber, F. *BBA* **1986**, *886*, 64−75.

(9) Ribi, H. O.; Reichard, P.; Kornberg, R. D. *Biochemistry* **1987**, *26*, 7974−7979.

(10) Metzger, J. W.; Sawyer, W. H.; Wille, B.; Biessert, L.; Bessler, W. G.; Jung, G. *BBA* **1993**, *1149*, 29−39.

(11) Haensler, J.; Schuber, F. *BBA* **1988**, *946*, 95−105.

(12) Spevak, W.; Nagy, J. O.; Charych, D. H.; Schaefer, M. E.; Gilbert, J. H.; Bednarski, M. D. *J. Am. Chem. Soc.* **1993**, *115*, 1146−1147.

(13) Martin, F. J.; Wayne, L. H.; Papahadjopulus, F. *Biochemistry* **1981**, *20*, 4229−4238.

(14) Egger, M.; Heyn, S.-P.; Gaub, H. E. *BBA* **1992**, *1104*, 45−54.

(15) Schmitt, L.; Dietrich, C.; Tampé, R. *J. Am. Chem. Soc.* **1994**, *116*, 8485−8491.

(16) Shnek, D. R.; Pack, D. W.; Sasaki, D. Y.; Arnold, F. H. *Langmuir* **1994**, *10*, 2382−2388.

(17) Uzgiris, E. E.; Kornberg, R. D. *Nature* **1983**, *301*, 125−129.

(18) Blankenburg, R.; Meller, P.; Ringsdorf, H.; Salesse, C. *Biochemistry* **1989**, *28*, 8214−8221.

(19) Mueller, W.; Ringsdorf, H.; Rump, E.; Wildburg, G.; Zhang, X.; Angermaier, L.; Knoll, W.; Liley, M.; Spinke, J. *Science* **1993**, *262*, 1707−1708.

(20) Savage, D.; Mattson, G.; Desai, S.; Nielander, G.; Morgensen, S.; Conklin, E. *Avidin-Biotin Chemistry: A Handbook*, 2nd ed.; Pierce Chemical Company: Rockford, IL, 1992.

S0002-7863(95)03937-0 CCC: $12.00

A more general concept would need a synthetic lipid containing an affinity ligand, somehow ubiquitous in binding to various proteins without additional modification or engineering steps. Because of its common use as energy source in nature, ATP seems to be the most prominent candidate. As known from affinity chromatography,[26] ATP covalently linked to the resin through its C8-[27,28] or N^6-position[29,30] of the adenine ring is favored for the purification of ATP-binding proteins, while ribose- or phosphate-linked ATP-resins[31] are less frequently used. The favorite binding of ATPase and protein kinases to C8- or N^6-modified ATP-resin can be explained by the related structure of their nucleotide binding pocket.[32] While the overall structure can vary from protein to protein, a loop is apparent in all of them, representing a sequence finger print. The sequences of this loop (Gly-X-X-Gly-X-Gly-Lys (Gly-loop) or Y_1-X-Y_2-Asp-X-Gly-Y_3-Y_3x-X-Y_4 (Y_n: groups of three to four particular residue types)) can be used to identify ATP-binding proteins based on sequence comparison.[33] The loop forms an anion hole, into which the triphosphate group complexed by divalent cations fits perfectly. Therefore, any modification of the phosphate groups often decreases the affinity, whereas modifications of the adenine ring can be tolerated to some extend. Prominent examples for proteins sharing this sequence motif are actin, F_1-ATPase, H-ras-p21, adenylate kinases, and heat shock proteins.

Here, we describe the synthesis and characterization of ATP-lipids linked via the C8- or N^6-position of the adenine ring to the lipid. The interchangeable concept allows the synthesis not only of either nonhydrolyzable or hydrolyzable ATP-lipids but also of ADP- and AMP-lipids. While the hydrolyzable ATP-lipids represent a self-organizing energy source in two dimensions, the nonhydrolyzable derivative can act as ligand for various ATP-binding proteins. To determine their biological activity, the ATP-lipids were first characterized by enzyme assays in micellar detergent solution. Using film balance techniques with epifluorescence microscopy[21,25] and phase contrast microscopy, we studied the properties of these ATP-lipids in lipid mono- and bilayers. Actin was chosen as model to investigate the specific docking of an ATP-binding protein to the ATP-lipid interface. Actin shares the basic principles of ATP-binding and can be purified by C8-linked ATP affinity chromatography. The strong interplay between coupling and decoupling of the actin network and the membrane is essential to maintain a high degree of softness or to induce shape transitions in cell membranes. However, these effects are still an enigma.[34] Also, the mechanism of domain formation and lateral organization is not understood. Therefore, the development of membranes supported by an actin network will be one approach to answer these questions ("phantom cells"). Due to the specific enrichment and orientation, this concept might also be applied for two-dimensional crystallization of ATP-binding proteins at ATP-lipid monolayers.

Materials and Methods

Materials. The following chemicals were used: DODA, lead(IV) acetate, ethylenediamine, and hexamethylenediamine (Fluka, Neu-Ulm, Germany), TR-DPPE (Molecular Probes, Oregon, USA), DMPC (Avanti Polar Lipids, Alabama, USA), Br-Ad, Cl-Ad, *o*-hydroxyphenylenephosphochloridate, methylenediphosphoric acid, diphosphoric acid tri-*n*-butylammonium salt, fluorescamine spray reagent, molybdenum blue spray reagent, and ornicol spray reagent (Aldrich, Steinheim, Germany). The enzyme assay kit for the C8-ATP analogues, proteins and chemicals for the N^6-ATP analogues assay, AMPPCP, and Triton X100 were ordered from Sigma (Deisenhofen, Germany). NBD-actin was prepared from rabbit muscle actin according to refs 35 and 36. TLC plates (Kieselgel 60 F_{254} and DIOL F_{254}), Kieselgel 60 (40−63 μm, 230−400 mesh), and LiChroPrep DIOL (40−63 μm, 60−230 mesh) were purchased from Merck (Darmstadt, Germany). All other solvents were from Fluka (Neu-Ulm, Germany) and were reagent *p.a.* grade or higher. Solvents were used without further purification unless otherwise stated. Prior to use triethylamine was refluxed over calcium hydride for 2 h and then destilled.

Lipid Characterization. Reactions were monitored by TLC (precoated plates 0.25 mm, silica gel F_{254}) and visualized by UV (aromatic groups), fluorescamine (primary amino groups), ornicol (*cis*-diol system in the ribose moiety), molybdenum blue (phosphate), and iodine (organic compound). Solvent ratios are given in volume/volume. For the solvent system chloroform/methanol/water/ammonia 65:25:2:2 an aqueous solution of 25% ammonia was used. The concentration of the Triton X100 solution is given in weight/volume. If necessary, products were purified by silica gel chromatography (LiChroPrep DIOL or silica gel 60). ^{1}H-NMR (500 MHz or 400 MHz) were recorded on a Bruker AM 500 or Bruker AM 400, respectively. ^{13}C-NMR (100 MHZ) and ^{31}P-NMR (161 MHz) were recorded on a Bruker AM 400. Chemical shifts (δ) are given in ppm relative to solvent as internal standard for ^{1}H- and ^{13}C-NMR and relative to 85% phosphoric acid as external standard for ^{31}P-NMR. MS (Finnigan, MAT, Forster City, CA, USA) was performed in the negative and positive ion mode. Phosphorus was determined according to ref 37. The given values are the average of two independent measurements. UV spectra were recorded on a Perkin-Elmer lambda 5 (Perkin-Elmer, Überlingen, Germany) after background correction and analyzed using the software provided by Perkin-Elmer.

Enzyme Assays. The ATPase activity of the C8-modified nucleotides was determined by the GADH/PGK assay (Sigma). 3-Phosphoglycerate is converted to 1,3-bis-phosphoglycerate by the PGK catalyzed reaction under ATP consumption. In the GADH-catalyzed reaction 1,3-bis-phosphoglycerate reacts subsequently to glycerinaldehyde-3-phosphate by reduction of NAD^+ to NADH. The activity of the N^6-modified nucleotides was analyzed by the HK/GPDH-coupled assay.[29] Glucose is converted to glucose-6-phosphate under consumption of ATP by the HK-catalyzed reaction. The glucose-6-phosphate is oxidized in the second step by the GPDH-catalyzed formation of $NADP^+$. Changes in A_{340} for both assays (increase or decrease) are proportional to the level of ATP. Each assay was performed with 100 nmol of nucleotide (0.14 mM, 700 μL of assay volume) which was estimated by the UV spectra using the molar extinction coefficients of 15.000 M^{-1} for ATP and AMPPCP,[38] 16.400 M^{-1} for C8-bromo-ATP,[38] 17.700 M^{-1} for C8-carboxyethylamino-, C8-aminoethylamino-ATP,[28] and DODA-HM-C8-AMPPCP/ATP **14b**,**c**, and 17.300 M^{-1} for N^6-carboxymethyl-ATP[30] and DODA-HM-N^6-AMPPCP/ATP **17b**,**c**. Buffers, substrates, and enzymes were used in concentration according to

(21) Dietrich, C.; Schmitt, L.; Tampé, R. *Proc. Nat. Acad. Sci. USA* **1995**, *92*, 9014−9018.
(22) Gritsch, S.; Neumaier, K.; Schmitt, L.; Tampé, R. *Biosensors & Bioelectronics* **1995**, 10, 805−812.
(23) Schmitt, L.; Bohanon, T. M.; Denzinger, S.; Ringsdorf, H.; Tampé, R. *Angew. Chem.* **1996**, *108*, 344−347.
(24) Gershon, P. D.; Khilko, S. *J. Immun. Meth.* **1995**, *183*, 65−76.
(25) Dietrich, C.; Boscheinen, O.; Scharf, K.-D.; Schmitt, L.; Tampé, R. *Biochemistry* **1996**, *35*, 1100−1104.
(26) Mosbach, K. *Adv. Emzymol.* **1978**, *46*, 205−278.
(27) Lee, C.-Y.; Lazarus, L. H.; Kabakoff, D. S.; Russell, P. J.; Laver, M.; Kaplan, N. O. *Arch. Biochem. Biophys.* **1977**, *178*, 8−18.
(28) Trayer, I. P.; Trayer, H. R.; Small, D. P.; Bottomley, R. C. *Biochem. J.* **1974**, *139*, 609−623.
(29) Guilford, H.; Larson, P.-O.; Mosbach, K. *Chem. Scr.* **1972**, *2*, 165−170.
(30) Lindberg, M.; Mosbach, K. *Eur. J. Biochem.* **1975**, *53*, 481−486.
(31) Haystead, C. M. M.; Gregory, P.; Sturgill, T. W.; Haystead, T. A. J. *Eur. J. Biochem.* **1993**, *214*, 459−467.
(32) Schulz, G. E. *Curr. Opin Struc. Biol.* **1992**, *2*, 61−67.
(33) Mimura, C. S.; Holbrook, S. R.; Ames, G. F.-L. *Proc. Natl. Acad. Sci. U.S.A.* **1991**, *88*, 84−88.
(34) Sackmann, E. *FEBS Lett.* **1994**, *346*, 3−16.
(35) Pardee, J. D.; Spudich, J. A. *Methods Enzymol.* **1982**, *85*, 164−181.
(36) Detmer, P.; Weber, A.; Elzinga, M.; Stephens, R. E. *J. Biol. Chem.* **1981**, *28*, 99−105.
(37) Zhou, X.; Arthur, G. *J. Lipid Res.* **1992**, *33*, 1233.
(38) Ikehara, M.; Uesugi, S. *Chem. Pharm. Bull.* **1969**, *17*, 348−352.

the manufacturer (Sigma) or to the literature.[30] The synthesized ATP-lipids were solubilized in 10% Triton X100 to analyze their specific activity. During a period of 10 min, the changes of A_{340} were recorded and normalized to the changes of the same concentration of ATP. The relative ATPase activity is determined from three independent measurements. The nonhydrolyzable ATP-lipids were characterized in competition assays using for the GADH/PGK or HK/GPDH assay for the C8- or N^6-modified AMPPCP-lipid, respectively. Here, a constant ATP concentration (100 nmol in 700 μL of volume) was assayed in the presence of an increasing molar ratio of competitor (0.01−100) which was solubilized in Triton X100. Changes of A_{340} were recorded over a period of 1 min.

Film Balance Measurements. The film balance unit consists of an epifluorescence microscope placed above a Langmuir trough (30 mm × 220 mm). The trough carries a subphase volume of 26 mL containing buffer A (10 mM HEPES, pH 7.5, 140 mM NaCl, 1 mM EDTA, 5 mM $MgCl_2$, 0.15 mM DTT) as described.[21] After spreading of the lipid mixture, the lateral pressure was adjusted by the surface area. NBD-actin was injected into the subphase via a small hole in the trough without touching and disturbing the air/water interface at 21.5 mN/m surface pressure. The surface tension was measured with a Wilhelmy system (accuracy ± 0.1 mN/m). For temperature control, peltier elements were placed below the base-plate (accuracy ± 0.2 °C). All experiments were performed at 20 °C at a surface pressure of 21.5 mN/m. Lipid monolayers were compressed with a rate of 3 Å^2/molecule × min. Compression, expansion, surface tension, and temperature are computer-controlled. The lateral distribution of the fluorescence-labeled lipids (TR-DPPE) and NBD-actin was imaged by means of an epifluorescence microscope mounted on a x-y translation stage. The fluorescence is detected with a SIT-camera (Hamamtsu, Hamamatsu, Japan). By changing adapted filters, various fluorescence dyes (NBD and TR) can be observed simultaneously.

Phase Contrast Microscopy. The setup consists of a modified, commercially available Zeiss Axiovert 10 with a magnification of 40×.[39] Images of the selected vesicle were taken with a charged coupled device (CCD) camera unit (Hamamatsu, C 3077/C 2400) and digitized as previously described.[40] The image processing software is based on the public domain program NIH Image. ATP-lipid containing vesicles were prepared as follows: 30 μL (15 mg/mL) of a DMPC solution (chloroform/methanol, 3/1) containing 1 mol% DODA-HM-C8-AMPPCP (**14b**) or DODA-HM-C8-AMP (**13b**) were placed onto the conducting sides of two ITO-deposited cover slides. After evaporation of the solvent in vacuum, the cover slides were placed in a specially developed chamber with the conducting sides facing each other. Unilamellar giant vesicles were obtained after electroswelling of the dried lipid film in buffer B (2 mM Tris, pH 7.5, 0.2 mM DTT, 0.2 mM $MgCl_2$) in the presence of 7 μg/mL actin for 2 h at 26 °C (1V amplitude and 10 Hz altering voltage).[41] Prior to use, actin was dialysed extensively against nucleotide-free buffer to remove any prebound nucleotide. The absence of ATP was determined by the GADH/PGK assay. Actin was desorbed from the outside of the vesicle by incubation of the vesicle solution with 0.4 mM EDTA, 2 mM Tris, pH 7.5 at 26 °C for 30 min.

Experimental Section

Synthesis of ATP-Lipids. Synthesis of 2′,3′-Isopropylidene-C8-bromoadenosine (Br-Ad-AC) 2. Br-Ad **1** (2.08 g, 6.01 mmol) was suspended in 35 mL of acetone and stirred after the addition of 3.40 g (18 mmol) of *p*-toluenesulfonic acid at room temperature until the solution became clear. The solution was neutralized with 1 M Na_2CO_3, and the aqueous phase extracted with chloroform until no UV absorption of the product at 263 nm was detected in the organic phase. The combined organic phases were dried over anhydrous sodium sulfate and solvent was removed in vacuum. Yield: 2.22 g (5.74 mmol) **2**; 96%. TLC: R_f (**2**) = 0.8 in $CHCl_3$/MeOH (9:1). UV: λ_{max} = 263 nm in DMSO. ^{1}H-NMR (400 MHz, DMSO): δ = 1.3 (s, 3H, (C**H**$_3$)$_2$C), δ = 1.5 (s, 3H, (C**H**$_3$)$_2$C), δ = 3.5 (m, 2H, H′-5, H″-5), δ = 4.2 (m, 1H, H′-4), δ = 5.0 (dd, 1H, H′-3), δ = 5.6 (dd, 1H, H′-2), δ = 6.0 (δ, 1H, H′-1), δ = 8.1 (s, 1H, H-8). ^{13}C-NMR (100 MHz, DMSO): δ = 25.2, 27.1 (**C**H$_3$C), δ = 61.5 (C′-5), δ = 79.1 (C′-3), δ = 81.7 (C′-2), δ = 87.1 (C′-4), δ = 90.9 (C′-1), δ = 113.2 ((CH$_3$)$_2$**C**), d = 119.3 (C-5), d = 126.3 (C-8), d = 149.7 (C-6), d = 152.8 (C-2), d = 155.1 (C-4). MS (FAB pos., $C_{13}H_{16}N_5O_4Br$): M + H$^+$ = 386.2 g/mol (^{79}Br isotope) M + H$^+$ = 388.2 g/mol (^{81}Br isotope), ratio: 100: 97.

Synthesis of 2′,3′-Isopropylidene-C8-bromoadenosine-5′-monophosphate-(*o*-hydroxyphenylester) (Br-AMP-AC-S) 3. Br-Ad-AC **2** (2.22 g, 5.74 mmol) was dissolved in 60 mL of absolute dioxane and stirred at room temperature for 3 h after the addition of 2.5 mL (21.90 mmol) of 2,6-lutidine and 1.21 g (6.32 mmol) of *o*-phenylene-phosphochloridate in 10 mL of absolute dioxane. The precipitated 2,6-lutidine hydrochloride was filtered off, and the reaction mixture was quenched by the addition of 60 mL of water. After adjusting the pH to 12 the mixture was stirred for 30 min. The aqueous phase was extracted with chloroform until no UV-absorption of the product at 263 nm was detected in the organic phase. After adjusting the pH to 1, the aqueous phase was again extracted with chloroform. The organic phases were combined and solvent removed in vacuum. Yield: 2.34 g (4.19 mmol) **3**; 73%. TLC: R_f (**3**) = 0.8 in $CHCl_3$/MeOH (1:1). UV: λ_{max} = 263 nm in DMSO. ^{1}H-NMR (400 MHz, DMSO): δ = 1.3 (s, 3H, (C**H**$_3$)$_2$C), δ = 1.5 (s, 3H, (C**H**$_3$)$_2$C), δ = 4.1 (m, 2H, H′-5, H″-5), δ = 4.3 (m, 1H, H′-4), δ = 5.1 (dd, 1H, H′-3), δ = 5.6 (dd, 1H, H′-2), δ = 6.0 (δ, 1H, H′-1), δ = 6.6 (m, 1H, phenyl-H-4), δ = 6.8 (m, 1H, phenyl-H-5), δ = 6.9 (m, 1H, phenyl-H-3), δ = 7.0 (m, 1H, phenyl-H-6), δ = 8.2 (s, 1H, H-8). ^{13}C-NMR (100 MHz, DMSO): δ = 25.2 ((**C**H$_3$)$_2$C), δ = 26.9 ((**C**H$_3$)$_2$C), δ = 65.6 (C′-5), δ = 79.1 (C′-3), δ = 81.3 (C′-2), δ = 85.6 (C′-4), δ = 90.7 (C′-1), δ = 113.2 ((CH$_3$)$_2$**C**), δ = 117.4 (phenyl C-4), d = 118.8 (phenyl C-5), d = 119.2 (C-5), d = 121.3 (phenyl C-3), d = 124.6 (phenyl C-6), d = 127.1 (C-8), d = 139.6 (phenyl C-2), d = 148.6 (phenyl C-1), d = 149.4 (C-6), d = 150.7 (C-2), d = 153.2 (C-4). ^{31}P-NMR (161 MHz, DMSO): d = 5.8 (s). MS (FAB neg., $C_{19}H_{21}N_5O_8PBr$): M − H$^+$ = 556.6 g/mol (^{79}Br isotope) M − H$^+$ = 558.6 g/mol (^{81}Br isotope), ratio: 100: 97.

Synthesis of 2′,3′-Isopropylidene-C8-bromoadenosine-5′-monophosphate (Br-AMP-AC) 4. Br-AMP-AC-S **3** (2.34 g, 4.19 mmol) was suspended in 160 mL of absolute dioxane and stirred at room temperature for 30 min after the addition of 2.61 g (5.87 mmol) of lead(IV) acetate. The reaction mixture was evaporated to dryness and subsequently dissolved in 110 mL of 10% aqueous triethylamine, pH 12.0. After 30 min the mixture was filtered and adjusted to pH 3.0. The aqueous phase was extracted with chloroform until the organic phase remained colorless, concentrated in vacuum, and lyophilized. Yield: 1.75 g (3.77 mmol) **4**; 90%. UV: λ_{max} = 263 nm in H_2O. ^{1}H-NMR (400 MHz, D_2O): δ = 1.3 (s, 3H, (C**H**$_3$)$_2$C), δ = 1.5 (s, 3H, (C**H**$_3$)$_2$C), δ = 3.6 (m, 2H, H′-5, H″-5), δ = 4.2 (m, 1H, H′-4), δ = 5.0 (1H, dd, H′-3), δ = 5.7 (1H, dd, H′-2), δ = 6.0 (d, 1H, H′-1), δ = 8.1 (s, 1H, H-8). ^{13}C-NMR (100 MHZ, D_2O): δ = 25.18 ((**C**H$_3$)$_2$C), δ = 26.99 ((**C**H$_3$)$_2$C), δ = 63.75 (C′-5), δ = 81.72 (C′-3), δ = 81.92 (C′-2), δ = 85.64 (C′-4), δ = 90.46 (C′-1), δ = 113.34 ((CH$_3$)$_2$**C**), δ = 119.13 (C-5), δ = 126.13 (C-8), δ = 149.84 (C-6), δ = 152.96 (C-2), δ = 154.92 (C-4). ^{31}P-NMR (161 MHz, D_2O): δ = 3.5 (s). MS (FAB neg., $C_{13}H_{17}N_5O_7PBr$): M − H$^+$ = 464.2 g/mol (^{79}Br isotope) M − H$^+$ = 466.2 g/mol (^{81}Br isotope), ratio: 100: 97.

Synthesis of 2′,3′-Isopropylidene-C8-(aminohexylamino)adenosine-5′-monophosphate (C8-HM-AMP-AC) 5b. Br-AMP-AC **4** (875 mg, 1.88 mmol) was dissolved in 75 mL of water and stirred at 130 °C for 2 h after the addition of 7.16 g (61.21 mmol) of hexamethylenediamine. After cooling to room temperature, the solution was diluted to 250 mL and purified using a linear gradient H_2O−1 M AcOH (total volume 2l) by anion exchange chromatography on Dowex AG1 × 8 (acetate form, 1 × 23 cm, flow rate 4 mL/min). Fractions containing the product were pooled, concentrated in vacuum, and lyophilized. Yield: 685 mg (1.37 mmol) **5b**; 73%. UV: λ_{max} = 278 nm in H_2O. ^{1}H-NMR (400 MHz, D_2O): δ = 1.3 (m, 7H, C**H**$_3$, Ad-NH(CH$_2$)$_2$-C**H**$_2$C**H**$_2$(CH$_2$)$_2$NH$_3^+$), δ = 1.5−1.6 (m, 5H, C**H**$_3$, Ad-NH(CH$_2$)$_4$C**H**$_2$-CH$_2$NH$_3^+$), δ = 2.6 (m, 4H, Ad-NH-CH$_2$C**H**$_2$(CH$_2$)$_2$C**H**$_2$CH$_2$NH$_3^+$), δ = 3.3 (m, 2H, Ad-NH-C**H**$_2$(CH$_2$)$_5$NH$_3^+$), δ = 3.5 (m, 2H, H′-5, H″-5), δ = 4.3 (m, 1H, H′-4), δ = 4.9 (dd, 1H, H′-3), δ = 5.4 (1H, dd, H′-2), δ = 6.3 (δ, 1H, H′-1), δ = 8.9 (s, 1H, H-8). ^{13}C-NMR (100 MHZ, D_2O): δ = 25.50 (**C**H$_3$), δ = 27.24 (**C**H$_3$), δ = 27.92 (C‴-4),

(39) Käs, J.; Sackmann, E.; Podgornick, R.; Svetina, S.; Zeks, B. *J. Phys. II France* **1993**, *3*, 631−645.

(40) Duwe, H. P.; Käs, J.; Sackmann, E. *J. Phys. France* **1991**, *51*, 945−962.

(41) Häckl, W. **1994** *Diploma Thesis*, Technical University Munich.

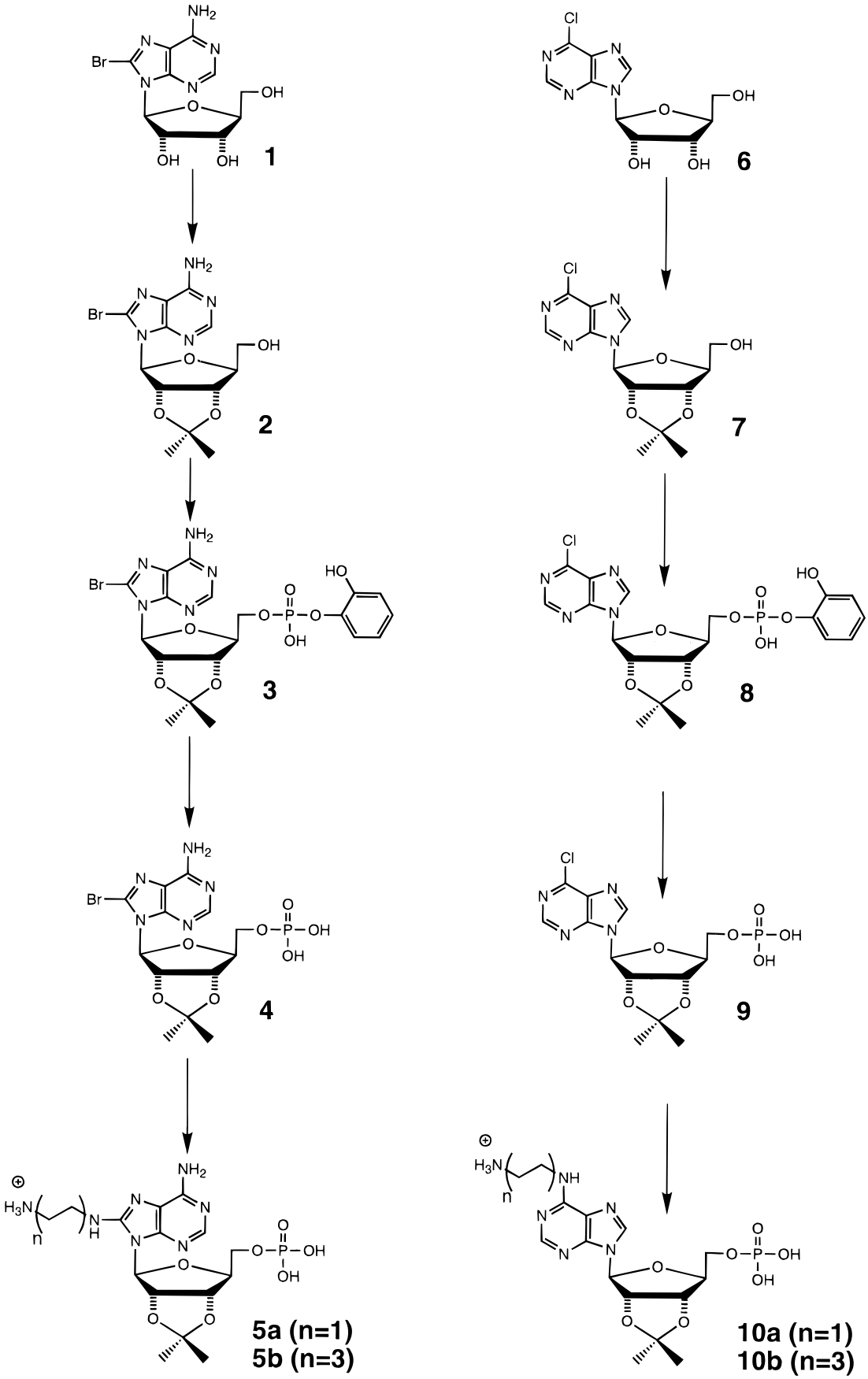

Figure 1. Synthesis of C8- (left lane) and N^6- (right lane) amino-modified 2′,3′-isopropylidene-adenosine-5′-monophosphates (AMP-AC). The spacer length can vary from ethylene ($n = 1$) to hexamethylene ($n = 3$).

$\delta = 28.25$ (C‴-5), $\delta = 29.38$ (C‴-3), $\delta = 30.84$ (C‴-6), $\delta = 42.21$ (C‴-2), $\delta = 45.15$ (C‴-1), $\delta = 67.12$ (C′-5), $\delta = 82.89$ (C′-3), $\delta = 83.87$ (C′-2), $\delta = 85.99$ (C′-4), $\delta = 91.08$ (C′-1), $\delta = 118.99$ (C-5), $\delta = 150.98$ (C-8), $\delta = 151.54$ (C-6), $\delta = 153.34$ (C-2), $\delta = 154.97$ (C-4). ^{31}P-NMR (161 MHz, D_2O): $\delta = 2.5$ (s). MS (FAB neg., $C_{19}H_{32}N_7O_7P$): $M - H^+ = 500.4$ g/mol.

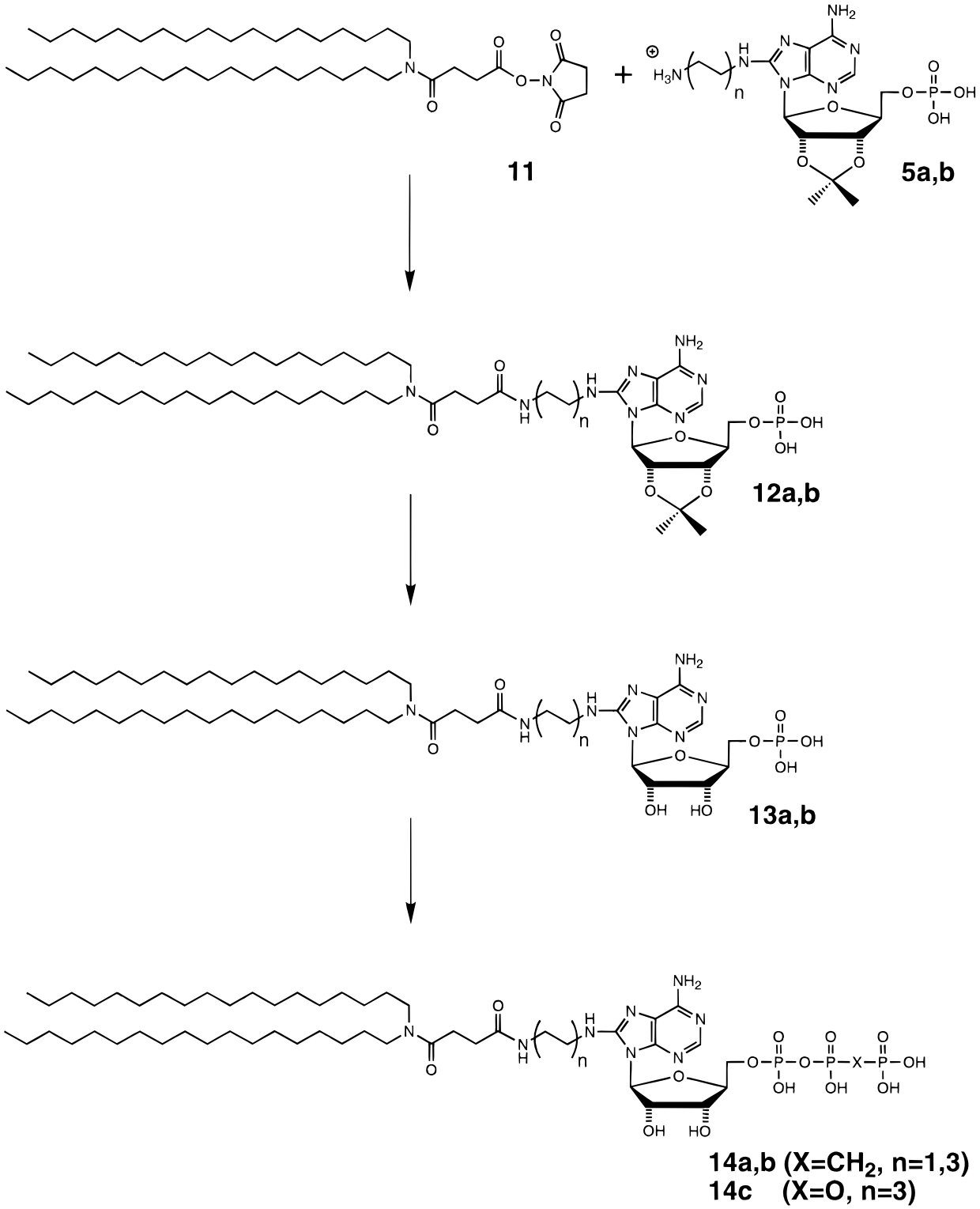

Figure 2. Synthesis of C8-modified nonhydrolyzable (X = CH_2, **14a,b**) and hydrolyzable (X = O, **14c**) ATP-lipids. The spacer length can vary from ethylene (n = 1) to hexamethylene (n = 3).

Synthesis of 2′,3′-Isopropylidene-C8-[((dioctadecyl)amino)succinylaminohexylamino]adenosine-5′-monophosphate (DODA-HM-C8-AMP-AC) 12b. DODA-Suc-NHS **11** (1.18 g, 1.63 mmol) was dissolved in 30 mL of absolute dioxane by heating at 40 °C and stirred at 70 °C over night after the addition of 1.17 mL (8.16 mmol) of absolute triethylamine and 685 mg (1.37 mmol) of C8-HM-AMP-AC **5b**. The reaction mixture was quenched by the addition of 20 mL of 1 M Na_2CO_3. The aqueous phase was extracted four times with chloroform. The combined organic phases were dried over anhydrous Na_2SO_4, and solvent was removed in vacuum. The product was purified by silica gel chromatography with $CHCl_3$/MeOH/H_2O/NH_3 (65:25:2:2). After removing the solvent in vacuum the product was crystallized from acetone. Yield: 1.03 g (0.93 mmol) **12b**; 68%. TLC: R_f (**12b**) = 0.6 in $CHCl_3$/MeOH/H_2O/NH_3 (65:25:2:2). UV: λ_{max} = 278 nm in $CHCl_3$/MeOH (3:1). ^{1}H-NMR (400 MHz, $CDCl_3$/MeOD 3:1): δ = 0.75 (t, 6H, C**H**$_3$), δ = 1.15 (m, 60H, $CH_3(CH_2)_{15}CH_2CH_2N$), δ = 1.3 (m, 7H, $(CH_2)_{15}CH_2CH_2N$, $(CH_3)_2C$), δ = 1.4 (m, 4H, $NH(CH_2)_3(CH_2)_2$-CH_2NH-Ad), δ = 1.5 (m, 5H, $NH(CH_2)_2CH_2(CH_2)_3$NH-Ad, $(CH_3)_2C$), δ = 2.3 (t, 2H, $NCOCH_2CH_2CONH$), δ = 2.45 (t, 2H, $NCOCH_2CH_2$-CONH), δ = 3.0 (dm, 6H, CH_2NCO, $CONHCH_2$), δ = 3.2−4.5 (m, 7H, not assignable), δ = 5.0 (dd, 1H, H′-3), δ = 5.2 (dd, 1H, H′-2), δ = 5.8 (d, 1H, H′-1), δ = 7.9 (s, 1H, H-2). ^{13}C-NMR (100 MHz, $CDCl_3$/

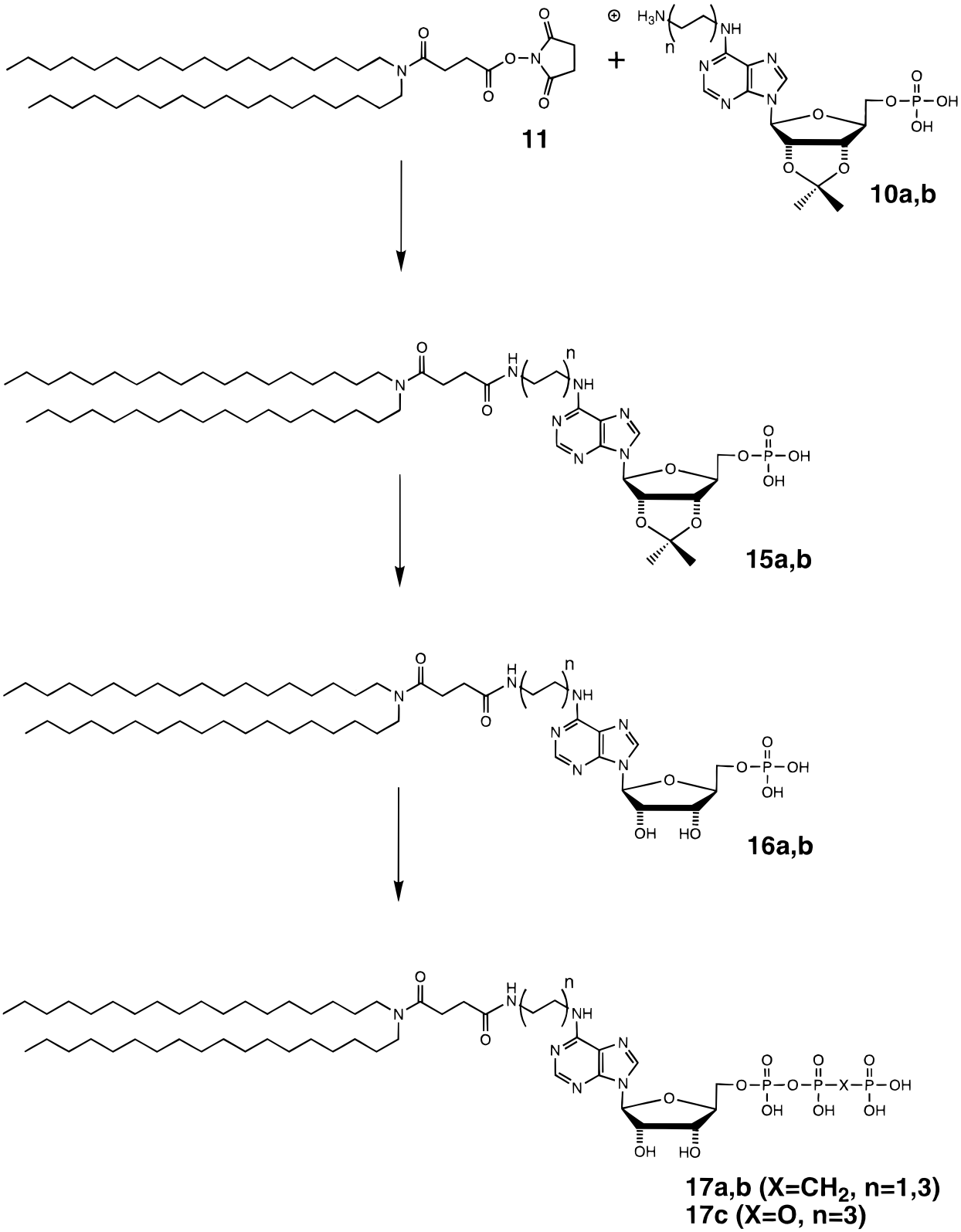

Figure 3. Synthesis of N^6-modified nonhydrolyzable (X = CH_2, **17a,b**) and hydrolyzable (X = O, **17c**) ATP-lipids. The spacer length can vary from ethylene (n = 1) to hexamethylene (n = 3).

MeOD 3:1): δ = 14.28, 23.00, 26.58, 26.69, 27.25, 27.39, 28.03, 28.93, 29.23, 29.69, 30.01, 31.50, 32.26 (CH_3(**C**H_2)$_{15}$$CH_2CH_2$N, HCH_2(**C**H_2)$_4$-CH_2NH-Ad, CO**C**H_2**C**H_2CO), δ = 39.69 (**C**H_2NCO), δ = 43.14 (CONH**C**H_2), δ = 63.75 (C′-5), δ = 70.28 (C′-3), δ = 72.09 (C′-2), δ = 84.69 (C′-4), δ = 88.21 (C′-1), δ = 115.42 (C-5), δ = 118.74 ((CH_3)$_2$**C**), δ = 143.42 (C-8), δ = 147.17 (C-6), δ = 149.17 (C-2), δ = 152.85 (C-4), δ = 172.46 (**C**O), δ = 173.58 (**C**O). ^{31}P-NMR (161 MHz, $CDCl_3$/MeOD 3:1): δ = 4.25 (s). MS (FAB neg, $C_{59}H_{109}N_8O_9P$): M − H^+ = 1103.9 g/mol.

Synthesis of C8-[((Dioctadecyl)amino)succinylaminohexylamino]-adenosine-5′-monophosphate (DODA-HM-C8-AMP) 13b. DODA-HM-C8-AMP-AC **12b** (1.03 g, 0.93 mmol) was dissolved in 75 mL of chloroform/methanol 1:1 and stirred at room temperature for 30 min after the addition of 6.5 mL of concentrated sulfuric acid. The solution was neutralized by the addition of 1 M Na_2CO_3, and the aqueous phase was extracted four times with chloroform. The organic layers were dried over anhydrous Na_2SO_4, solvent was removed in vacuum, and the product was crystallized from acetone. Yield: 887 mg (0.84 mmol)

Table 1. Relative ATPase Activity of DODA-HM-C8-ATP **14c**, DODA-HM-N^6-ATP **17c**, and Various C8- and N^6-Modified Nucleotides

nucleotides	relative ATPase activity [au]
ATP[a,b]	100%
C8-bromo-ATP[a]	36% ± 6%
C8-aminoethylamino-ATP[a]	65% ± 3%
C8-carboxyethylamino-ATP[a]	47% ± 9%
DODA-HM-C8-ATP **14c**[a]	56% ± 7%
N^6-carboxymethyl-ATP[b]	58% ± 10%
DODA-HM-N^6-ATP **17c**[b]	53% ± 8%

Experimental details are given in Materials and Methods: [a] GADH/PGK assay. [b] HK/GPDH assay.

13b; 90%. TLC: R_f (**13b**) = 0.4 in $CHCl_3$/MeOH/H_2O (65:25:4). UV: λ_{max} = 278 nm in $CHCl_3$/MeOH (9:1). Phosphorus: 1.2 ± 0.15 mol:mol adenine. ^{1}H-NMR (400 MHz, $CDCl_3$/MeOD 3:1): δ = 0.75 (t, 6H, C**H**$_3$), δ = 1.15 (m, 60H, $CH_3(CH_2)_{15}CH_2CH_2N$), δ = 1.3 (m, 4H, $(CH_2)_{15}CH_2CH_2N$), δ = 1.4 (m, 4H, $NH(CH_2)_3(CH_2)_2CH_2NH$-Ad), δ = 1.5 (m, 2H, $NH(CH_2)_2CH_2(CH_2)_3NH$-Ad), δ = 2.3 (t, 2H, $NCOCH_2CH_2CONH$), δ = 2.45 (t, 2H, $NCOCH_2CH_2CONH$), δ = 3.0 (dm, 6H, CH_2NCO, $CONHCH_2$), δ = 3.2−4.5 (m, 7H, not assignable), δ = 5.0 (dd, 1H, H′-3), δ = 5.2 (dd, 1H, H′-2), δ = 5.8 (d, 1H, H′-1), δ = 7.9 (s, 1H, H-2). ^{13}C-NMR (100 MHz, $CDCl_3$/MeOD 3:1): δ = 8.84 (**C**H$_3$), δ = 14.28, 23.00, 26.58, 26.69, 27.25, 27.39, 28.03, 28.93, 29.23, 29.69, 30.01, 31.50, 32.26 ($CH_3(CH_2)_{15}CH_2CH_2N$, $NHCH_2(CH_2)_4CH_2NH$-Ad, $COCH_2CH_2CO$), δ = 39.69 (CH_2NCO), δ = 43.14 ($CONHCH_2$), δ = 63.75 (C′-5), δ = 70.28 (C′-3), δ = 72.09 (C′-2), δ = 84.69 (C′-4), δ = 88.21 (C′-1), δ = 115.42 (C-5), δ = 143.42 (C-8), δ = 147.17 (C-6), δ = 149.17 (C-2), δ = 152.85 (C-4), δ = 172.46 (**C**O), δ = 173.58 (**C**O). ^{31}P-NMR (161 MHz, $CDCl_3$/MeOD3:1): δ = 4.25 (s). MS (FAB neg, $C_{56}H_{105}N_8O_9P$): M − H$^+$ = 1063.8 g/mol.

Synthesis of C8-[((Dioctadecyl)amino)succinylaminohexylamino]-adenosine-5′-[β,γ-methylene-triphosphate] (DODA-HM-C8-AMP-PCP) 14b. DODA-HM-C8-AMP **13b** (118 mg, 0.11 mmol) was dissolved in 2 mL of HMPTA and stirred over night at room temperature after the addition of 95 μL (0.22 mmol) of tri-*n*-octylamine and 35 μL (0.17 mmol) diphenyl chlorophosphate. To remove reactive phosphorylation reagent the mixture was stirred for additional 2 h at 10^{-2} mbar at room temperature. After the addition of 40 mg (0.22 mmol) of methylenediphosphoric acid and 190 μL (0.44 mmol) tri-*n*-octylamine, the mixture was stirred for 2 h at 60 °C. After quenching the solution with 10 mL of chloroform and 10 mL of water, the aqueous phase was extracted five times with chloroform. Combined organic phases were dried over anhydrous Na_2SO_4 and solvent was removed in vacuum. The product was purified by silica gel chromatography (LiChroPrep DIOL) using a step gradient from chloroform to chloroform/methanol (9:1) and finally chloroform/methanol/water (2:3:1). The product was eluted with chloroform/methanol/water (2:3:1) and pooled, and solvent was removed in vacuum. Yield: 43 mg (35 μmol) **14b**; 32%. TLC: R_f (**14b**) = 0.9 in $CHCl_3$/MeOH/H_2O (2:3:1) on silica DIOL plates. UV: λ_{max} = 278 nm in $CHCl_3$/MeOH (3:1). Phosphorus: 2.8 ± 0.2 mol:mol adenine.

Results

Activity of ATP-Lipids in Micellar Solution. Self-assembled hydrolyzable and nonhydrolyzable ATP-lipids represent an energy source or a competitor for various ATP-hydrolyzing enzymes in two dimensions. Therefore, activities of the C8- or N^6-modified nucleotide analogues were analyzed by the GADH/PGK assay or the HK/GPDH assay, respectively. To avoid any steric hindrance due to self-organization, the ATP-lipids were first characterized in micellar solution of Triton X100. This nonionic detergent by itself does not influence both assays up to concentration of 15% (data not shown). The activities of the hydrolyzable ATP-lipids are summarized in Table 1. DODA-HM-C8-ATP **14c** carries an activity of 56% ± 7% and DODA-HM-N^6-ATP **17c** of 53% ± 8%. Note, that the same concentration of ATP represents 100% activity. Within the range of error, the data are in very good agreement with those measured for various other C8-modified nucleotides (ranging from 36% for C8-Br-ATP up to 65% for C8-aminoethylamino-ATP) and N^6-modified nucleotides (58% for N^6-carboxymethyl-ATP), indicating that the lipid-linked nucleotides are fully active and accessible for different ATP-hydrolyzing enzymes.

Table 2. IC_{50} Values for AMPPCP, DODA-HM-C8-AMPPCP **14b**, and DODA-HM-N^6-AMPPCP **17b** Determined in a Competition Assay

nucleotides	IC_{50} [molar excess]
AMPPCP[a]	1.3 ± 0.003
DODA-HM-C8-AMPPCP **14b**[a]	1.9 ± 0.3
AMPPCP[b]	1.4 ± 0.004
DODA-HM-N^6-AMPPCP **17b**[b]	1.2 ± 0.3

Experimental details are given in Materials and Methods: [a] GADH/PGK assay. [b] HK/GPDH assay.

The activity of the nonhydrolyzable ATP-lipids (DODA-HM-C8-AMPPCP **14b** and DODA-HM-N^6-AMPPCP **17b**) were studied in a competition assay using nonhydrolyzable AMPPCP as reference. The IC_{50} values of these nonhydrolyzable ATP-lipids are summarized in Table 2. A 1.9- or 1.2-fold molar excess of the C8- or N^6-modified AMPPCP-lipid is needed for 50% inhibition of the ATPase activity. These IC_{50} values are in agreement to those obtained for AMPPCP (1.3 and 1.4 for both assays). In summary, the activities of the hydrolyzable as well as nonhydrolyzable ATP-lipids are comparable to their free counterparts in micellar solution.

Activity of ATP-Lipids in Self-Assembled Monolayers. Next, we characterized the two-dimensional properties of the synthesized ATP-lipids. The nonhydrolyzable ATP-lipid (DODA-HM-C8-AMPPCP, **14b**) was used as model compound and spread from organic solution at the air−water interface. As shown by area-pressure isotherms, the pure ATP-lipid monolayer is stable during several cycles of expansion and compression up to 20 mN/m. But, because of the electrostatic repulsion of the highly negatively charged lipid head group, the pure monolayer collapsed around 25 mN/m. Interestingly, the isotherms are strongly dependent on the presence or absence of Mg^{2+} in the subphase (data not shown).

To increase the stability of the ATP-lipid monolayer and to avoid any steric hindrance during protein binding, the nonhydrolyzable ATP-lipid was diluted by the matrix lipid DMPC. DMPC/DODA-HM-C8-AMPPCP (**14b**) (16 nmol) (9:1 mol:mol, doped with 0.2 mol% TR-DPPE) was spread on subphase buffer A. This monolayer is stable up to 30 mN/m. It can be compressed and expanded several times without observing changes of the area-pressure isotherms. To investigate the specific docking of an ATP-binding protein to this functionalized ATP-lipid layer, we chose actin as a model compound. It has been speculated that polymerization and depolymerization of actin in proximity to membranes is responsible for cell shape, adhesion, and movement. Because of the high surface activity of actin (about 20 mN/m), the ATP-lipid monolayer was compressed to 21.5 mN/m. After equilibration over night, 1.6 nmol fluorescence-labeled actin (NBD-actin) was injected yielding an equimolar protein/ATP-lipid ratio (55 pM). It is important to note that actin is free of any prebound ATP as determined by the GADH/PGK assay. As shown in Figure 4a, the surface pressure increased about 1 mN/m within 40 min after protein injection. In addition, we observed a significant change in the phase behavior and fluidity of the ATP-lipid monolayer by epifluorescence microscopy. Before protein injection, a phase separation of the lipid mixture occurred around 20 mN/m leading to small, round-shaped domains which aggregate to clusters. After protein injection, these clusters were nearly completely redistributed forming isolated round-shaped

domains. In addition, the monolayer became rigid and the fluidity of the lipid monolayer was drastically reduced as observed by photobleaching experiments.

The same experiment was carried out in the presence of 0.1 mM AMPPCP as competitor (Figure 4b). In contrast to the first experiment, only a slight increase in the surface pressure of 0.2 mN/m was detected after protein injection, indicating that binding of actin can be blocked specifically by a nonhydrolyzable nucleotide. The slight increase of the surface pressure can be explained either by an unspecific absorption of NBD-actin or by an exchange reaction between free and lipid-anchored nucleotide. In addition, we performed a control experiment under identical conditions using an AMP-lipid monolayer (Figure 4c). In the case of a DMPC/DODA-HM-C8-AMP (**13b**) (9:1 mol:mol) monolayer, no interaction with the ATP-binding protein was observed. In the last two control experiments (Figure 4b,c), we could not detect any changes of the fluorescence micrographs (Texas-Red and NBD) or of the dynamic properties of the monolayer after protein injection. The fluorescence micrographs of NBD-actin differ only if the protein was injected in the absence of the competitor. While in this case the NBD-actin was enriched at the ATP-lipid interface, no fluorescence-labeled protein was detected in the presence of the competitor (data not shown). Since docking of an ATP-binding protein can be specifically blocked by AMPPCP and since the charges of the AMPPCP-lipid complexed by Mg^{2+} and the AMP-lipid are identical, an electrostatic interaction can be excluded.

Immobilization of Actin at ATP-Lipid Containing Vesicles. The monolayer experiments demonstrate that actin is specifically attached to the membrane by ATP-lipids as protein anchor. Whereas the lipid monolayer represents an ideal model to study recognition processes at the lipid interface, vesicles are commonly used as model for cell membranes. In this study, giant unilamellar DMPC vesicles which are in the order of 10 μm were prepared in the presence of monomeric actin (7 μg/mL) by electroswelling. These vesicles were doped with 1 mol% DODA-HM-C8-AMPPCP (**14b**) or DODA-HM-C8-AMP (**13b**), respectively. Due to the specific interaction with the nonhydrolyzable ATP-lipid, the attached actin layers stabilize the membrane. In consequence, drastic changes on the viscoelastic properties of the membrane such as bending modes, thermal undulations, and shape transitions were observed by phase contrast microscopy.

Figure 5 summarizes the situation when actin is bound onto both sides of the lipid vesicle. Increasing the temperature from 26 °C to 37 °C, these actin-stabilized vesicles run through three distinct states: (i) Below 29.9 °C, spherical vesicles are observed (Figure 5a,b). In contrast to actin-free vesicles which show a very dynamic behavior in this temperature range, no thermal undulations of the actin-stabilized vesicles were detected. In this case, although the temperature is above the main phase transition temperature of the matrix lipid DMPC (24.3 °C), the membrane is very rigid due to the attached actin layer. (ii) Increasing the temperature above 29.9 °C, the spherical vesicles turn into edged forms with straight lines (Figure 5c−e, indicated by arrows). Especially, the shape at 31.0 °C (Figure 5e) is energetically completely disfavored for a pure lipid bilayer. These stress-induced forms can only be explained by a protein layer attached to both sides of the vesicle. (iii) Above 36.0 °C, round-shaped vesicle are recovered. But now, the vesicles are very dynamic which is indicated by thermal undulations of the bilayer (data not shown). This dynamic behavior is similar to an actin-free DMPC vesicle and can be explained by an irreversible thermal denaturation of the adsorbed actin layer. After cooling and reheating no protein-induced stabilization was observed. Figure 5f describes schematically the situation where an actin layer is attached inside and outside of the ATP-lipid containing vesicle.

Since Mg^{2+} is essential for ATP-binding of ATPases and kinases, the outer actin-network was removed by complexing Mg^{2+} with EDTA. In this case, the membrane is only stabilized by an actin layer at the inside of the vesicle. Due to this asymmetric situation, the transitions between the different vesicle states are observed at lower temperatures. Angular forms were induced already at 26.3 °C (Figure 6b). In addition, these locally restricted undulations resulted in a budding process directed only to the outside (Figure 6c−e, indicated by arrows). The irreversible transition of the free, round-shaped vesicles occurred also at lower temperature (30.6 °C). Figure 6f summarizes schematically the asymmetric situation where the actin layer outside of the vesicle is removed by incubation with EDTA.

In order to exclude the possibility that this process is guided by unspecific, electrostatic interactions of actin with the negatively charged membrane interface, vesicles containing 1 mol% DODA-HM-C8-AMP (**13b**) were prepared under identical conditions. In this case, no influence of the protein onto the viscoelastic properties of the bilayer were observed (data not shown). Both shape transitions and thermal undulations are comparable to an actin-free, pure DMPC vesicle.

Discussion

As shown in Figure 1, the protected C8- and N^6-amino modified nucleotides C8-AE/HM-AMP-AC **5a**,**b** and N^6-AE/HM-AMP-AC **10a**,**b** were synthesized starting from Br-Ad **1** and Cl-Ad **6**. Although the direct phosphorylation of the primary 5′-hydroxyl group without protecting secondary alcohols (2′, 3′-OH) is described,[42−44] the method of Reese et al.[45] using *o*-phenylenephosphochloridate as phosphorylating agent in the presence of the protected diol system was found superior in yield, simplicity of purification, and cleavage of the phosphate protecting groups in contrast to similar reactions using 2,2,2-tribromoethylphosphoromorphilinochloridate[46] or di(2-*tert*-butylphenyl)phosphochloridate.[47] In the former reaction, the proposed selective phosphorylation concerning 5′-OH selectivity failed. The conversion of the nucleosides Br-Ad **1** and Cl-Ad **6** to the corresponding 2′,3′-isopropylidene derivatives Br-Ad-AC **2** and Cl-Ad-AC **7** was achieved by standard protocols.[48,49] The phosphorylation of both protected nucleosides Br-Ad-AC **2** and Cl-Ad-AC **7** was performed in the presence of a slight excess of the phosphorylation reagent and of the sterically hindered base 2,6-lutidine at room temperature. The phosphotriester was quenched by water and stirring at pH 12 for several minutes at room temperature. The phosphodiesters Br-AMP-AC-S **3** and Cl-AMP-AC-S **8** were converted into the monoesters Br-AMP-AC **4** and Cl-AMP-AC **9** by oxidative removal of the *o*-hydroxyphenylester using lead(IV) acetate in organic solution and fragmentation of the intermediate in alkaline solution at room temperature.[50] All products could easily be isolated by extraction. In summary, the synthetic route leads to the nucleotides in moderate yields without time-consuming purification steps. It can easily be expanded to large

(42) Yoshikawa, M.; Kato, T.; Takenishi, T. *Bull. Chem. Soc. Jap.* **1969**, *42*, 3505−3508.
(43) Sowa, T.; Ouchi, S. *Bull. Chem. Soc. Jpn.* **1975**, *48*, 2084−2090.
(44) Imai, K.-I.; Fuji, S.; Takanohashi, K.; Furukawa, Y.; Masuda, T.; Honjo, M. *J. Org. Chem.* **1969**, *34*, 1547−1550.
(45) Khwaja, T. A.; Reese, C. B.; Stewart, J. C. M. *J. Chem. Soc. (C)* **1970**, 2092−2100.
(46) van Boom, J. H.; Crea, R.; Luyten, W. C.; Vink, A. B. *Tetrahedron Lett.* **1975**, *32*, 2779−2782.
(47) Hes, J.; Mertes, M. P. *J. Org. Chem.* **1974**, *25*, 3767−3769.
(48) Greene, T. W. *Protective Groups in Organic Chemistry*; Wiley-Interscience: New York, 1981.
(49) Hampton, A. *J. Am. Chem. Soc.* **1961**, *83*, 3640−3645.
(50) Warren, C. D.; Jeanloz, R. W. *Biochemistry* **1972**, *11*, 2565−2572.

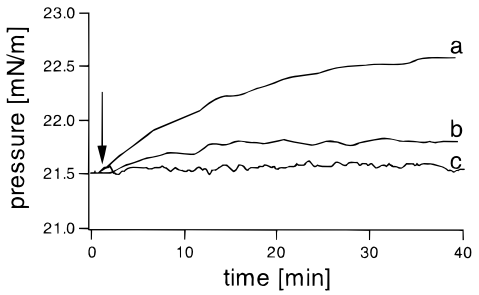

Figure 4. Time-dependent changes of the surface pressure of a DMPC/DODA-HM-C8-AMPPCP **14b** (9:1 mol:mol, doped with 0.2 mol% TR-DPPE) monolayer after protein injection. Lipid (16 nmol) was spread on buffer A. The monolayer was compressed to 21.5 mN/m and equilibrated over night. NBD-actin (1.6 nmol) was injected into subphase buffer A yielding a final concentration of 55 pM (arrow). All experiments were carried out under identical experimental conditions with the exception of: (a) protein injection in the absence of free nucleotides in buffer A, (b) protein injection in the presence of 0.1 mM AMPPCP in buffer A, and (c) protein injection to a DMPC/DODA-HM-C8-AMP **13b** (9:1 mol:mol, doped with 0.2 mol% TR-DPPE) in the absence of free nucleotides in buffer A.

scale preparations. In the last step the halogen-nucleotide-monophosphates Br-AMP-AC **4** and Cl-AMP-AC **9** were amino-functionalized by nucleophilic substitution leading to C8-AE/HM-AMP-AC **5a**,**b**[28] and N^6-AE/HM-AMP-AC **10a**,**b**,[30] respectively.

As known from biotin-lipids,[51] DNA gyrase/lipid interaction,[52] or hapten-lipids[53] the spacer length between lipid backbone and ligand is a crucial point in protein-ligand interaction and the formation of two-dimensional protein crystals at functionalized lipid interfaces.[53] In our approach this variability is introduced in the amino-functionalization step. Here, we chose only two possibilities, ethylenediamine and hexamethylenediamine. The last one is widely used and often the optimal choice as known from biotin-lipid systems[54] or ATP-affinity columns.[26] But, in principle, any diamine including polyethylene glycol derivatives can be used.

In the final step, the C8- and N^6-modified nucleotides (C8-AE/HM-AMP-AC **5a**,**b** (Figure 2) and N^6-AE/HM-AMP-AC **10a**,**b** (Figure 3)) were coupled to the carboxy-activated lipid DODA-Suc-NHS **11**.[15] Several methods are known in literature for the cleavage of the acetal in the resulting DODA-AE/HM-C8-AMP-AC **12a**,**b** and DODA-AE/HM-N^6-AMP-AC **15a**,**b**, respectively.[55−57] All of these methods failed due to either incomplete cleavage or side reactions. Without any side reactions, the isopropylidene group was cleaved only by concentrated sulfuric acid in chloroform/methanol (1:1).[48] DODA-C8-AE/HM-AMP **13a**,**b** and DODA-AE/HM-N^6-AMP **16a**,**b** were characterized by TLC, UV, ^{1}H-, ^{13}C-, ^{31}P-NMR, and MS. A separate activation step is necessary to convert these AMP-lipids into ATP-lipids (DODA-AE/HM-C8-AMPPCP **14a**,**b**, DODA-HM-C8-ATP **14c** and DODA-AE/HM-N^6-AMP-PCP **17a**,**b**, DODA-HM-N^6-ATP **17c**). Surprisingly, only a few methods exist for this purpose that include the activation with dicyclohexylcarbodiimide,[58] carbonyldiimidazolide,[59] dibutyl phosphinothioic bromide,[60] and diphenylphosphochloridate.[61,62] Because of the limited solubility of the AMP-lipids in DMF or DMSO, the best results were obtained by the activation with diphenylphosphochloridate.[61] Furthermore, HMPTA instead of DMF/dioxane or DMF/$CHCl_3$ as solvent promotes the activation of the AMP-lipids and their conversion to ATP-lipids which is in line with other studies.[63] Without the isolation of the activated compound, the ATP-lipids were formed by reaction with diphosphoric acid.

In contrast to all AMP-lipids, which could be characterized by ^{1}H-, ^{13}C-, and ^{31}P-NMR, line-broadening (around 0.5 ppm for ^{1}H-NMR and around 5 ppm for ^{31}P-NMR) was observed for the triphosphate nucleotide derivative. Various ratios of chloroform/methanol or addition of TFA did not improve the NMR spectra. Therefore, the determination of phosphorus[37] versus adenine (determined by UV-absorption) in combination with the detected UV-maxima and TLC visualized with iodine (alkyl chain), ornicol (ribose moiety), and molybdenum blue (phosphorus) on silica DIOL was used to characterize the ATP-lipids. Noteworthy, the ATP-lipids are hydrolyzed on non-modified silica plates catalyzed by the acidic reactive surface.

Beside the described synthesis, we reconsidered various other synthetic routes to prepare ATP-lipids. Following alternative pathways, we synthesized various C8-functionalized ATP analogues via C8-bromo-ATP[38] starting from ATP. Bromine was finally substituted by ethylenediamine[27] or β-alanine.[64] The N^6-modified ATP derivatives were generated by the reaction of β-propiolactone[65] or ethylenimine[66] with ATP under acidic conditions and subsequent Dimroth-rearrangement in basic solution. The C8- and N^6-modified nucleotides were condensed with carboxy- or amino-functionalized lipids using active ester chemistry in organic solution. In the case of amino-functionalized ATP-derivatives, only low yields of ATP-lipids were obtained, while in the case of carboxy-functionalized ATP-derivatives no product formation was observed. Alternatively, we tried to phosphorylate adenosine lipids in organic solution. Br-Ad and Cl-Ad were converted to the corresponding C8- and N^6-modified nucleosides by substitution of the halogen atoms with ethylene- and hexamethylenediamine, respectively and condensed with DODA-Suc-NHS. As mentioned above, a selective phosphorylation of the adenosine-lipids in organic solution such as chloroform or methylenechloride without protection of the 2′,3′-diol positions failed completely.[42,44] After protection, the phosphorylation by 2,2,2-tribromoethyl-phosphoromorphilinochloridate[46] or di(2-*tert*-butylphenyl)phosphochloridate[47] brought up problems due to the incomplete cleavage of the phosphate protecting groups. In the case of phosphorylchloride[42] side-reactions were observed.

In summary, this elaborated route which can be transferred in principle to other nucleotides and lipid derivatives opens up a wide range of possibilities to synthesize not only ATP-lipids but also ADP-lipids, AMP-lipids, and more important various nonhydrolyzable triphosphates.

Because of the limited accessibility of functionalized lipids in vesicles, we characterized the function of the ATP-lipids in

(51) Hoffmann, M.; Müller, W.; Ringsdorf, H.; Rourke, A. M.; Rump, E.; Suci, P. A. *Thin Solid Films* **1992**, *210*, 780−783.
(52) Brisson, A.; Olofsson, A.; Ringler, P.; Schmutz, M.; Stoylova, S. *Biol. Cell* **1994**, *80*, 221−228.
(53) Kimura, K.; Arata, Y.; Yasuda, T.; Kinosita, K.; Nakanishi, M. *J. Immunology* **1990**, *69*, 323−328.
(54) Darst, S. A.; Ahlers, M.; Meller, P. H.; Kubalek, E. W.; Blankenburg, H.; Ribi, H. O.; Ringsdorf, H.; Kornberg, R. D. *Biophys. J.* **1991**, *59*, 387−396.
(55) Huet, F.; Lechevallier, A.; Pellet, M.; Conia, J. M. *Synthesis* **1978**, 63−65.
(56) Tewson, T. J.; Welch, M. J. *J. Org. Chem.* **1978**, *43*, 1090−1092.
(57) Guindon, Y.; Yoakim, C.; Morton, H. E. *J. Org. Chem.* **1984**, *49*, 3912−3920.
(58) Moffat, J. G. *Can. J. Chem.* **1964**, *42*, 599−604.
(59) Hoard, D. E.; Ott, D. G. *J. Am. Chem. Soc.* **1965**, *87*, 1785−1788.
(60) Hata, T.; Furusawa, K.; Sekine, M. *J. Chem. Soc.* **1975**, 196−197.
(61) Michaelson, A. M. *BBA* **1964**, *91*, 1−13.
(62) Cramer, F.; Wittmann, R. *Chem. Ber.* **1960**, *94*, 331−340.
(63) Ott, D. G.; Kerr, V. N.; Hansbury, E.; Hayes, F. N. *Anal. Biochem.* **1967**, *21*, 469−472.
(64) Chan, P. H.; Hassid, W. Z. *Anal. Biochem.* **1975**, *64*, 372−379.
(65) Zappelli, A.; Rossodivita, A.; Prosperi, G.; Pappa, R.; Re, L. *Eur. J. Biochem.* **1976**, *62*, 211−215.
(66) Bückmann, F.; Wray, V. *Biotech. Appl. Biochem.* **1992**, *15*, 303−310.

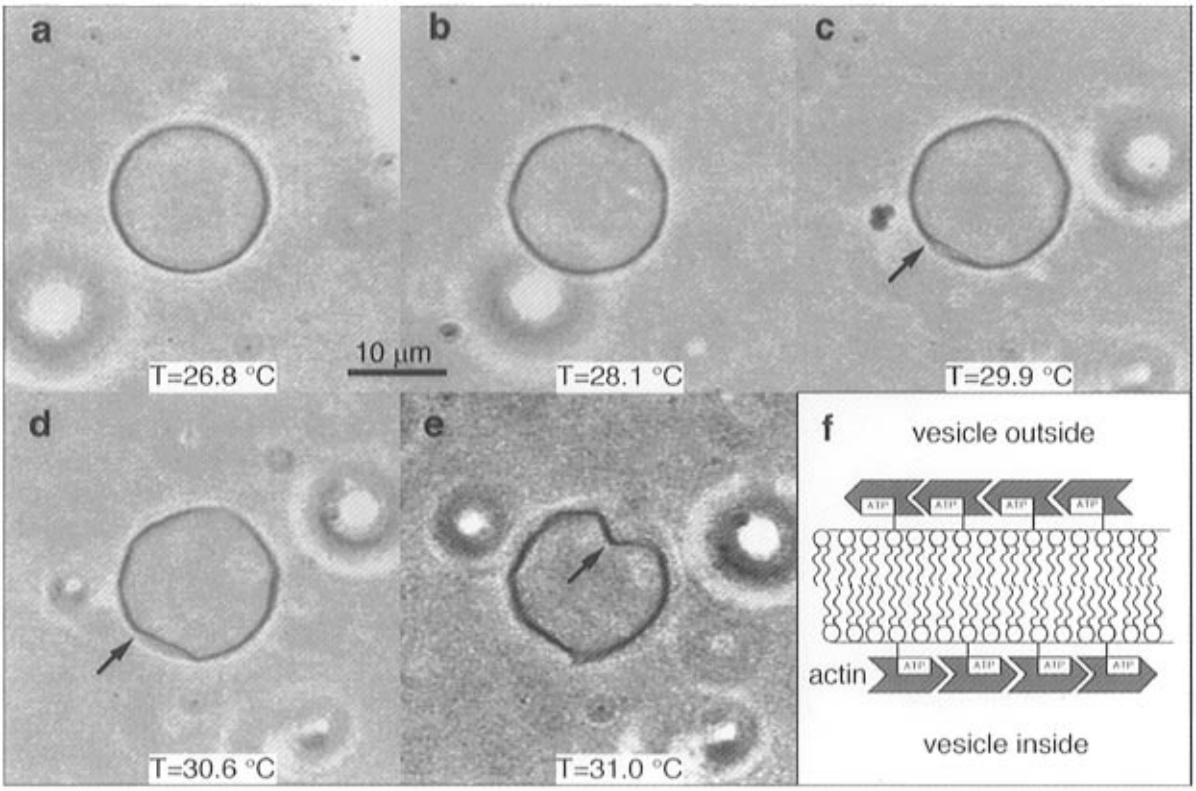

Figure 5. Phase contrast micrographs of a giant unilamellar DMPC vesicle containing 1 mol% DODA-HM-C8-AMPPCP (**14b**) at various temperatures. Vesicles were prepared in the presence of 7 μg/mL actin. Images were recorded and digitized as described in Materials and Methods.

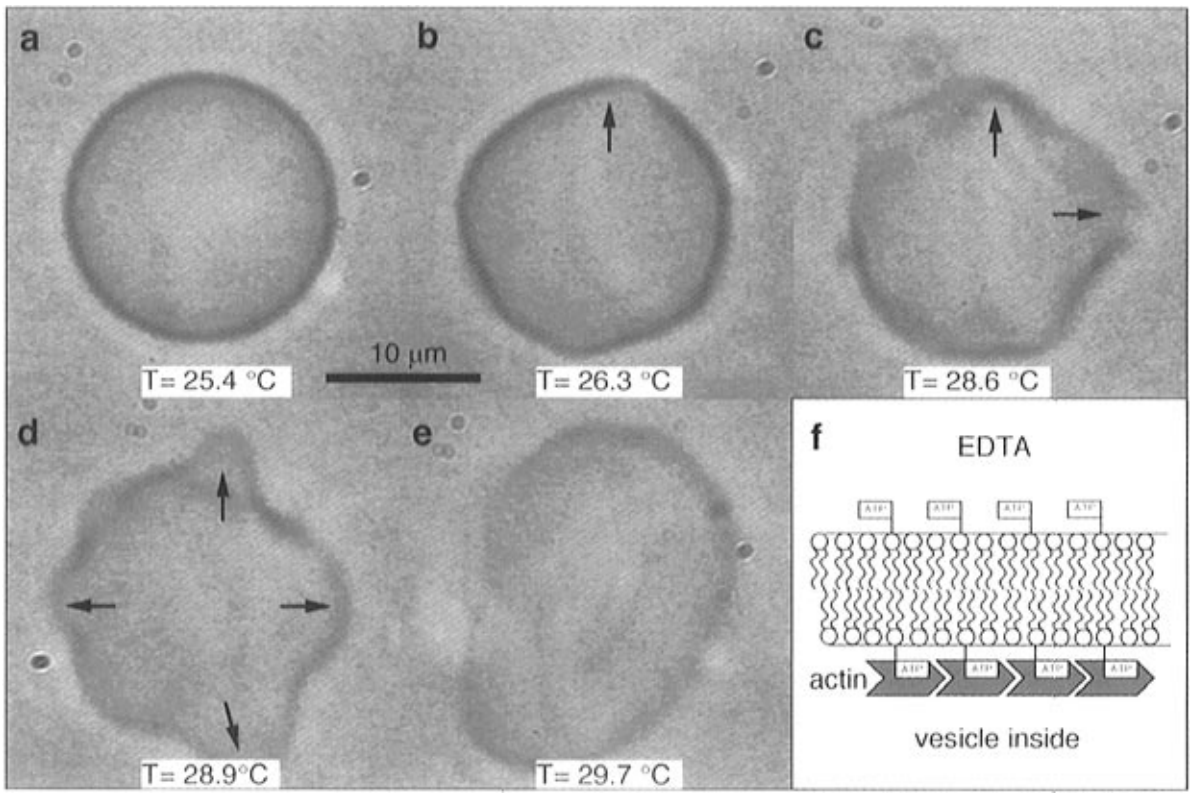

Figure 6. Phase contrast micrographs of a giant unilamellar DMPC vesicle containing 1 mol% DODA-HM-C8-AMPPCP (**14b**) at various temperatures after incubation with 0.4 mM EDTA, 2 mM Tris, pH 7.5 for 30 min. Images were recorded and digitized as described in Materials and Methods.

detergent solution where each ATP-lipid is highly diluted in detergent micelles (Tables 1 and 2). While the aggregation number of Triton X100 micelle is around 140,[67] the nucleotide-lipids are strongly diluted to one molecule per ten micelles in both assays (0.14 mM ATP-lipid, 10% Triton X100). In the case of the C8- and N^6-modified ATP-lipids, the GADH/PGK and HK/GPDH assay was used, respectively. Two assays were needed because modifications of the adenine system affect the conformation of the nucleotide.[68,69] Thereby the affinity of these

(67) Deutscher, M. P. *Methods Enzymol.* **1990**, *182*, 247.

(68) Evans, F. E.; Lee, C. Y.; Kapmeyer, H.; Kaplan, N. O. *Bioorg. Chem.* **1978**, *7*, 57−67.

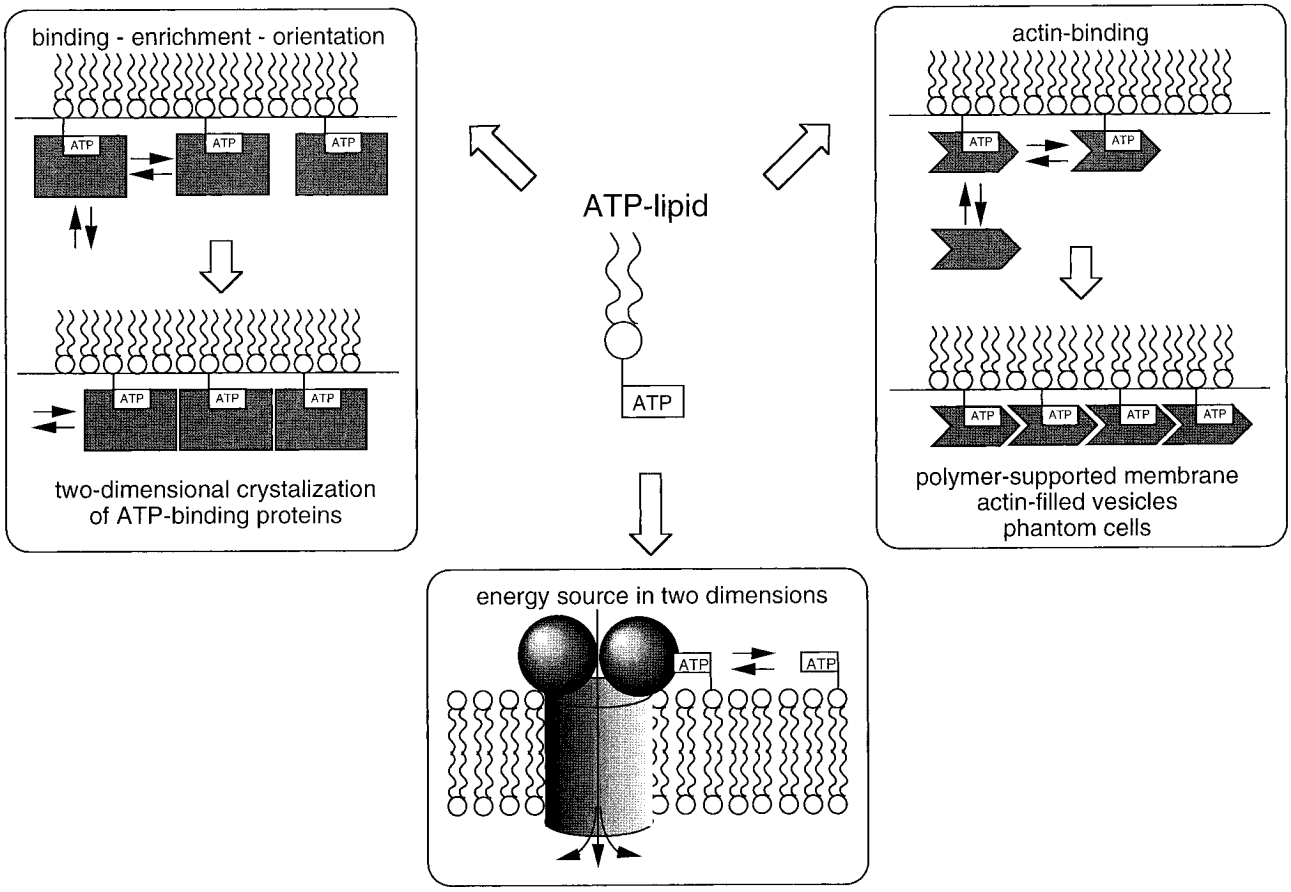

Figure 7. Possible applications of the novel class of ATP-lipids (schematic illustration).

modified ATP-analogues to various ATPases and kinases is changed. PGK represents one example for this sensitive behavior.[29] As shown in Table 1 modification of the adenine ring of ATP reduces the biological activity of those C8-ATP analogues. The reduction of the activity relative to ATP ranges from 36% for Br-ATP,[38] 42% for C8-carboxyethylamino-ATP[65] to 65% for C8-aminoethylamino-ATP.[27] The value for DODA-HM-C8-ATP **14c** of 47% is in agreement with the values of the C8-modified nucleotides. The activity of the solubilized DODA-HM-N^6-ATP (53%) is comparable with N^6-carboxymethyl-ATP (58%).[70] Next, the nonhydrolyzable ATP-lipids (**14b** or **17b)** were used as competitors in the corresponding enzyme assays. A 1.9- or 1.2-fold molar excess of C8- or N^6-modified AMPPCP-lipid (**14b** or **17b**) is needed for 50% inhibition of the ATPase activity, respectively. These IC_{50} values fit to those obtained for AMPPCP indicating that the lipid-anchored nucleotides are as active and accessible as free AMPPCP.

In the second step, the binding behavior of actin to a nonhydrolyzable ATP-lipid monolayer was investigated at the air−water interface. As shown in Figure 4, the binding of NBD-actin strongly depends on the presence or absence of nonhydrolyzable ATP in the subphase. No interaction of NBD-actin with an AMP-lipid monolayer was found under identical experimental conditions. Note, that the AMP-lipid and AMP-PCP-lipid complexed by Mg^{2+} have the same net charge at neutral pH. The slight increase of the surface pressure (<0.2 mN/m) is more likely due to an exchange reaction of actin between free and lipid-bound nucleotides than an unspecific interaction. In lipid mixtures which contain positively charged lipids an electrostatic interaction of the negatively charged actin with these monolayers induces a drastic increase of the surface pressure (20 mN/m) below a so-called "critical pressure".[71] This interaction, which is explained by a penetration of actin into the monolayer, depends on the amount of positively charged lipids within the layer. In our system, an increase of only 1 mN/m was detected. The film balance measurements are supported by fluorescence microscopy: While a diffuse fluorescence of NBD-actin and drastic decrease in membrane fluidity was observed after protein injection in the absence of competitor, no changes were detected in its presence. The immobilization of the ATP-binding proteins is mediated by the nucleotide head group. Therefore, we can exclude an unspecific electrostatic interaction.

Finally, the behavior of a lipid-protein composite generated by the specific immobilization of actin to ATP-lipid containing vesicles was studied by phase contrast microscopy.[72] This method have been successfully applied to determine thermal undulations, shape transitions, and the viscoelastic properties of vesicles.[73] As shown in Figure 5, ATP-lipid containing vesicles prepared in the presence of actin revealed a physical behavior completely different to actin-free vesicles.[39] The shape of these thermally stressed vesicles can only be explained by a fixation of the bilayer from both sides by an adsorbed protein layer.

It has to be stressed that spontaneous polymerisation of actin in solution can be excluded under these conditions. But, based

(69) Sarma, R. H. L.; C.-H.; Evans, F. E.; Yathindra, N.; Sundaralingam, M. *J. Am. Chem. Soc.* **1974**, *96*, 7337−7348.
(70) Sakamoto, H.; Nakamura, A.; Urabe, I.; Yamada, Y.; Okada, H. *J. Ferment. Technol.* **1986**, *64*, 511−516.
(71) Grimard, R.; Tancréde, Giquaud, C. *BBRC* **1990**, *190*, 1017−1022.
(72) Cortese, J.; Schwab, B.; Frieden, C.; Elson, E. *Proc. Nat. Acad. Sci. U.S.A.* **1989**, *86*, 5773−5777.
(73) Menger, F. M.; Gabrielson, K. D. *Ang. Chem.* **1995**, *107*, 2260−2278.

on the specific binding, the interfacial concentration of actin is drastically increased, resulting in a two-dimensional concentration higher than the critical concentration needed for polymerization.[36] At this stage, polymerization can be further promoted by a conformational change caused by the binding of actin to the ATP-lipid. ATP-hydrolysis is only required for the depolymerization step.[74] Therefore, the specific immobilization can result in additional protein−protein interactions. In a rough estimation the ATP-lipid possess an area of around 50 Å^2. Consequently, actin must cover an area of around 5000 Å^2 to explain the membrane stabilization only by specifically bound protein. Based on the X-ray structure of monomeric actin, it requires an area of around 1500 Å^2.[75] Thus, the strong interaction can be explained either by long-range interaction or by the incorporation of additional monomeric actin not directly bound to the ATP-lipid. It has to be determined whether the formed protein-layer is somehow similar to F-actin. A detailed analysis of the adsorbed protein layer and the physical state of the vesicles is in progress.

Our interpretation of an ATP-lipid induced formation of an actin layer is further supported by experiments in the presence of EDTA (Figure 6). Due to its charge, EDTA is not able to diffuse across a lipid bilayer. As a result, the adsorbed actin layer at the outside of the vesicle is removed, whereas the inside layer is not affected. In comparison to the case where the vesicles are stabilized from both sides, the transition between different vesicle shapes and the irreversible desorption of the protein layer is shifted to lower temperatures (from 29.9 °C to 26.3 °C for stressed vesicles and from 36.0 °C to 30.6 °C for free vesicles). In addition, the budding process which is only directed to the outside of the vesicle demonstrates that the stressed membranes are only stabilized from one side by the actin layer (Figure 6c,d).

In this study, we have described the synthesis and characterization of ATP-lipids. This universal, self-assembling ligand allows the biofunctionalization of interfaces without biotinylation steps or genetic engineering techniques. Some potential aspects of this novel class of ATP-lipids are summarized schematically in Figure 7. As shown by film balance experiments, actin interacts specifically with an ATP-lipid monolayer. In eukaryotic cells, the actin network is anchored at the membrane via specific proteins. The assembly and disassembly of this polymer network are driven by ATP. The experiments with ATP-lipid containing vesicles indicate that actin is trapped at the interface by specific binding to nonhydrolyzable ATP-lipid forming a protein network. Such polymer-supported membranes should be a realistic model to mimic shape transitions of membranes mediated by the attached cytoskeleton network ("phantom cells") or the mechanism controlling the softness of cell membranes.[34] In supported lipid layer, this biocompatible network can preserve the essential dynamic properties of reconstituted membrane proteins preventing protein interaction with the solid support.[76,77] Furthermore, based on their two-dimensional characteristics, ATP-lipids can act as energy source for ATP-dependent membrane proteins addressing the topology of ATP-binding sites. Due to the universality of the ATP-ligand in nature, a vast variety of ATP-binding proteins should be specifically bound, enriched, and oriented at these ATP-lipid interfaces that is one of the essential steps in two-dimensional protein crystallization at functionalized lipid monolayers.

Acknowledgment. We are indebted to Walter Häckl for expert assistance with the vesicle experiments and Dr. E. Sackmann for helpful and critical discussions concerning the "flicker" experiments. The excellent help for providing NMR and MS spectra of Dr. I. Zetl, Dr. J. Sonnenbichler, and Dr. W. Schäfer (NMR and MS research units) at the Max-Planck-Institut für Biochemie (Martinsried) are gratefully acknowledged. We thank Karin Scharpf for the preparation of NBD-actin, and Klaus Neumaier, Almuth Berisch, and Annette Kloboucek for discussion and technical assistance concerning film balance measurements. Fritz Bückmann (GBF, Braunschweig) is gratefully acknowledged for the first steps in nucleotide chemistry. This work was supported by the Deutsche Forschungs Gemeinschaft (grant Ta 157/1).

Supporting Information Available: A detailed description, R_f values, ^{1}H-, ^{13}C-, ^{31}P-NMR, and MS data of all synthesized compounds (23 pages). See any current masthead page for ordering information.

JA953937M

(74) Weisenberg, R. C.; Deery, W. J. *Nature* **1976**, *263*, 792−793.
(75) Kabsch, W.; Mannherz, H. G.; Suck, D.; Pai, E. F.; Holmes, K. *Nature* **1990**, *347*, 37−44.
(76) Kühner, M.; Tampé, R. Sackmann, E. *Biophys. J.* **1994**, *67*, 217−226.
(77) Dietrich, D.; Tampé, R. *BBA* **1995**, *1238*, 183−191.

(78) Abbreviations: A: Absorption; abs.: absolute; ADP: adenosine-5′-diphosphate; AcOH: acetic acid; AMP: adenosine-5′-monophosphate; AMPPCP: β,γ-methylene-adenosine-5′-triphosphate; ATP: adenosine-5′-triphosphate; Br-Ad: C8-bromo-adenosine; Br-Ad-AC: 2′,3′-isopropylidene-C8-bromo-adenosine; Br-AMP-AC-S: 2′,3′-isopropylidene-C8-bromo-adenosine-5′-monophosphate-(*o*-hydroxy-phenylester); Br-AMP-AC: 2′,3′-isopropylidene-C8-bromoadenosine-5′-monophosphate; C8-AE-AMP-AC: 2′,3′-isopropylidene-C8-aminoethylaminoadenosine-5′-monophosphate; C8-HM-AMP-AC: 2′,3′-isopropylidene-C8-aminohexyl-aminoadenosine-5′-monophosphate; Cl-Ad: N^6-chloro-purine-riboside; Cl-Ad-AC: 2′,3′-isopropylidene-N^6-chloro-purine-riboside; Cl-AMP-AC-S: 2′,3′-isopropylidene-N^6-chloro-purine-riboside-5′-monophosphate-(*o*-hydroxy-phenylester); Cl-AMP-AC: 2′,3′-isopropylidene-N^6-chloro-purine-riboside-5′-monophosphate; DMF: dimethylformamide; DMPC: 1,2-dimyristoyl-*sn*-glycerol-phosphocholine; DMSO: dimethyl sulfoxide; DODA-AE-C8-AMP-AC: 2′,3′-isopropylidene-C8-[((dioctadecyl)amino)-succinylaminoethylamino]adenosine-5′-monophosphate; DODA-AE-C8-AMP: C8-[((dioctadecyl)amino)succinylaminoethylamino]adenosine-5′-monophosphate; DODA-AE-C8-AMPCP: C8-[((dioctadecyl)amino)succinylaminoethylamino]adenosine-5′-[β,γ-methylene-triphosphate]; DODA-AE-C8-ATP: C8-[((dioctadecyl)amino)succinylaminoethylamino]-adenosine-5′-triphosphate; DODA-AE-N^6-AMP-AC: 2′,3′-isopropylidene-N^6-[((dioctadecyl)amino)succinylaminoethyl]adenosine-5′-monophosphate; DODA-AE-N^6-AMP: N^6-[((dioctadecyl)amino)succinyl-aminoethyl]adenosine-5′-monophosphate; DODA-AE-N^6-AMPCP: N^6-[((dioctadecyl)amino)succinyl-aminoethyl]-adenosine-5′-[β,γ-methylene-triphosphate]; DODA-AE-N^6-ATP: N^6-[((dioctadecyl)amino)succinylaminoethyl]adenosine-5′-triphosphate; DODA-HM-C8-AMP-AC: 2′,3′-isopropylidene-C8-[((dioctadecyl)amino)succinylaminohexylamino]adenosine5′-monophosphate; DODA-HM-C8-AMP: C8-[((dioctadecyl)amino)succinyl-aminohexylamino]-adenosine-5′-monophosphate; DODA-HM-C8-AMPCP: C8-[((dioctadecyl)amino)succinylaminohexylamino]adenosine-5′-[β,γ-methylenetriphosphate]; DODA-HM-C8-ATP: C8-[((dioctadecyl)-amino)succinylaminohexylamino]adenosine-5′-triphosphate; DODA-HM-N^6-AMP-AC: 2′,3′-isopropylidene-N^6-[((dioctadecyl)amino)succinyl-aminohexyl]adenosine-5′-monophosphate; DODA-HM-N^6-AMP: N^6-[((dioctadecyl)amino)succinylaminohexyl]adenosine-5′-monophosphate; DODA-HM-N^6-AMPCP: N^6-[((dioctadecyl)amino)succinylaminohexyl]-adenosine-5′-[β,γ-methylenetriphosphate]; DODA-HM-N^6-ATP: N^6-[((dioctadecyl)amino)succinylaminohexyl]adenosine-5′-triphosphate; DODA-Suc-NHS: N-[(hydroxysuccinimidyl)succinyl]dioctadecylamine; DODA: dioctadecylamine; DTT: dithiothreitrol; EDTA: ethylenediaminetetraacetic acid; FAB: fast atomic bombardement; GADH: glycerinaldehyde-3-phosphate dehydrogenase (E.C. 1.2.1.12); GPDH: glucose-6-phosphate dehydrogenase (E.C. 1.1.1.49); HEPES: *N*-(2-hydroxyethyl)-piperazine-*N*′-2-ethanesulfonic acid; HMPT: hexamethylphosphoric triamide; HK: hexokinase (E.C. 2.7.1.1); IC_{50}: inhibitor concentration needed for 50% competition; ITO: indium-tin oxide; MS: mass spectrometry; NADH: nicotinamide-adenine dinucleotide (reduced form); NADP: nicotinamide-adenine dinucleotide-3′-phosphate (oxidized form); N^6-AE-AMP-AC: 2′,3′-isopropylidene-N^6-aminoethyladenosine-riboside-5′-monophosphate; N^6-HME-AMP-AC: 2′,3′-isopropylidene-N^6-aminohexyl-adenosine-riboside-5′-monophosphate; NBD: 7-nitrobenzo-2-oxo-1,3-diazole; N^6-HM-AMP-AC: 2′,3′-isopropylidene-N^6-aminohexyl-adenosine-riboside-5′-monophosphate; NMR: nuclear magnetic resonance; PGK: phosphoglycerate kinase (E.C. 2.7.2.3); TFA: trifluoroacetic acid; TLC: thin-layer chromatography; TR-DPPE: *N*-(TexasRed)-1,2-dipalmitoyl-*sn*-glycerol-ethanolamine; UV: ultraviolet.